Turkish Journal of Mathematics

Volume 48 | Number 5 Article 10

9-10-2024

Comprehensive computational study on transient heat transfer in functionally graded longitudinal fins under time-varying laser heating

HÜSEYİN DEMİR

İNCİ ÇİLİNGİR SÜNGÜ

İBRAHİM KELEŞ

TÜBİTAK

Turkish Journal of Mathematics

http://journals.tubitak.gov.tr/math/

Research Article

Turk J Math
(2024) 48: 941 – 954

doi:10.55730/1300-0098.3551

Comprehensive computational study on transient heat transfer in functionally graded longitudinal fins under time-varying laser heating

Hüseyin DEMİR[1], **İnci ÇİLİNGİR SÜNGÜ**[2,*], **İbrahim KELEŞ**[3]
[1]Department of Software Engineering, Faculty of Engineering and Natural Sciences, Samsun University, Samsun, Turkiye
[2]Department of Education of Mathematics and Sciences, Faculty of Education, Ondokuz Mayıs University, Samsun, Turkiye
[3]Department of Mechanical Engineering, Faculty of Engineering and Natural Sciences, Samsun University, Samsun, Turkiye

Received: 05.06.2024 • **Accepted/Published Online:** 05.08.2024 • **Final Version:** 10.09.2024

Abstract: The present study assumes that the material properties of the fin vary by a force rule in the axial direction, with the exception of the thermal relaxation coefficient, which is assumed to be constant. The temperature distribution in the longitudinal fin with homogeneous cross-section exposed to the laser heat source is numerically investigated. This is because these constraints lead to a linear differential equation with partial solutions that cannot be analytically resolved using conventional methods, except for a few elementary order functions. Consequently, a linear or nonlinear system of equations as a function of time is obtained by transforming a differential equation attained with one or more independent factors using the highly efficient, potent, and practical semianalytical method known as the Chebyshev pseudospectral method. Temperature distributions in the fin are then examined in terms of different homogeneity factors and time-varying heat source capacity. Furthermore, the numerical solutions' convergence is emphasised, and the results are confirmed using homogeneous solutions from the literature.

Key words: Transient heat transfer, functionally graded materials, laser heat source, Chebyshev pseudospectral method

1. Introduction

Fins with circular, concave, convex, and rectangular profiles are developed and engineered to achieve higher thermal performance when utilized as heat transfer components within many engineering applications. These fins require proper heat treatment tailored to their intended environments. Lasers are preferred as heat sources for this process due to their ability to generate intense radiation pulses suitable for surface thermal treatment [6, 24, 30]. Laser techniques are also chosen for their overall cost-effectiveness compared to traditional methods. Additionally, lasers apply minimal heat to the workpiece, which improves surface properties, such as hardness. To successfully achieve the desired hardened layer depth, the laser's energy efficiency and processing time must be carefully selected. Therefore, understanding the distribution of environmental temperatures is essential to reaching the targeted hardened depth and maximum surface temperature.

So as to study the heat transfer in fins and the patterns of heat flow via expanded surfaces for steady state, many assumptions have been made for an accurate and numerical analysis. There is a clear closed-form

*Correspondence: icilingir@omu.edu.tr
2010 *AMS Mathematics Subject Classification:* 65M70, 80AXX

solution for temperature distributions and efficiency in various fins with an expanded surface discovered in the literature [10, 13] using these reasonable assumptions. Furthermore, there are numerous studies in the literature about the productivity and efficiency of longitudinal fins, along with the optimisation of their size and profile [2–4, 11, 15–17, 20–23, 28, 29]. Basically, the longitudinal fin's temperature distribution leads to the development of mechanical flaws like fatigue and cracks, which shorten the fin's lifespan because of various expansions. Therefore, understanding this temperature distribution is crucial for selecting the appropriate material and fin type during the design process [14]. By applying numerical or perturbation approaches in addition to analytical methods, it is possible to determine the temperature distributions on the fins for both steady state and transient state [1, 7–9, 14, 17, 19, 20, 25].Rapid technological advancements have made it possible to design with materials that are not only long-lasting and highly durable but also capable of gradually altering their properties. These substances are called functionally graded materials (FGM) since they exhibit gradual change and may be chosen over composite substances. Due to their superior resistance compared to other materials, FGMs have gained widespread use in various climates and conditions. Numerous studies in the literature have documented the effects of these materials across different engineering fields where they are applied [9, 13, 17, 26, 28]. These investigations are relevant to thermal performance and reverse engineering applications, which analyse the transient behaviour of temperature distribution in gradually graded longitudinal fins. While the authors investigated the temperature distribution and transient response for the FGM longitudinal-shaped fin, they assumed the density and specific heat to remain constant. In contrast, previous studies have reported that thermal conductivity varies gradually across different forms of fin materials. As a result, this research is significant for studying the behaviour of longitudinal FGM fins under the influence of a laser heat source in a transient state. It assumes that thermal conductivity, density, and specific heat vary exponentially in the axial direction, while excluding the thermal relaxation parameter. Despite their advantageous properties, FGMs may become deformed in long-term operating environments.

To address these deformations, lasers with inexpensive, accurate, and rapid processing capabilities are employed. Consequently, the impact of the laser source on FGMs is inevitable. This article aims to demonstrate the transient thermal behaviour of a longitudinal-shaped fin made of FGMs under the influence of a time-varying laser heat source, while maintaining a constant cross-sectional area. The transient thermal efficiency of a longitudinal fin composed of FGMs was studied, considering that the fin had an adiabatic tip. The axial route assumes exponential changes in the body's material characteristics, with the exception of the thermal relaxation value, which is considered to remain constant. An internal heat source is implemented via laser heating. These conditions lead to a nonhomogeneous linear differential equation. Since this problem cannot be solved analytically, it is resolved mathematically using the Chebyshev pseudospectral method (CPM), which is a method that can resolve variable coefficient boundary value problems with high performance. The CPM, a semianalytical method, can be used to convert a differential equation derived from one or more unrelated factors into a system of linear or nonlinear equations [5, 12, 27]. Because of its high accuracy, simplicity of usage, and capacity to employ both a tough mesh in the path of the centre points and a tight mesh near the border, the CPM was selected as the ideal method for this investigation.

2. Governing equations

Consider a longitudinally functionally graded straight airfoil with profile area (A). The cross-sectional perimeter is denoted by (P) and the distance by (b) (see e.g. [9]). Convectional heat transfer coefficient (h) at the fin outside is steady and the fin is primarily in thermal balance with the receiver at the warmth (T_s). Except for

the thermal relaxation coefficient, the fin's material properties are assumed to fluctuate exponentially in the axial direction, while the interior heat source is a transitory laser heating. The blade base temperature changes gradually from (T_s) to (T_b) at $(t \geq 0)$ even though the tip is still adiabatic.

The partial differential formula that calculates the FGM thermal conductivity of the convective fin's temperature response is as follows [17]:

$$\frac{\partial}{\partial X}\left[k(X)\frac{\partial T}{\partial X}\right] - \frac{hP}{A}[T - T_s] + g(X,t) = \rho(X)c(X)\frac{\partial T}{\partial t}, \quad 0 < X < b \tag{1}$$

where (g) is the energy source term, (c) is the definite heat capacity, and (ρ) is density. This is represented as [18]:

$$g(X,t) = I(t)(1-R)\mu \exp(-\mu X) \tag{2}$$

where (μ) is the absorption coefficient, (R) is the body's outside reflectivity, and $(I(t))$ is the laser incidence concentration.

At the outset and in the boundary conditions,

$$T(X,0) = T_s \tag{3}$$

$$T(b,t) = T_b \tag{4}$$

$$\frac{\partial T}{\partial X}(0,t) = 0 \tag{5}$$

The material properties of the FGM fin are assumed to change exponentially in the axial direction, while the thermal relaxation coefficient is considered constant.

$$k(X) = k_0 exp(aX), \quad c(X) = c_0 exp(aX), \quad \rho(X) = \rho_0 exp(aX) \tag{6}$$

where a is the inhomogeneity parameters and k_0, ρ_0, and c_0 represent the medium's material characteristics at $X = 0$, and k represents the thermal conductiveness. The following explains how dimensionless variables are defined:

$$x = \frac{X}{b}, \quad \tau = \frac{k_0}{(\rho_0 c_0 b^2)}t, \quad \theta = \frac{T - T_s}{T_b - T_s}, \quad N_c = \frac{hPb^2}{Ak_0} \tag{7}$$

After nondimensionalization, the main problem is reduced to the partial differential formula found below.

$$\frac{\partial \theta}{\partial \tau} = aexp(-ax)\frac{\partial \theta}{\partial x} + exp(-ax)\frac{\partial^2 \theta}{\partial x^2} - exp(-2ax)N_c\theta + exp(-2ax)G(x,\tau) \tag{8}$$

$$G(x,\tau) = g_0\eta(\tau)exp(-\mu x) \tag{9}$$

$$g_0 = \frac{b^2(1-R)\mu I_r}{k_0(T_b - T_s)}, \quad \eta(\tau) = \frac{I(\frac{\rho_0 c_0 b^2}{k_0}\tau)}{I_r}$$

Considering the fundamental and border conditions,

$$\theta(x,0) = 0, \quad \theta(0,\tau) = 1, \quad \frac{\partial \theta}{\partial x}(0,\tau) = 0 \tag{10}$$

Internal source term $G(x,\tau)$ get three different cases [18]

$g_0 = 0$ -no internal source

1. $\mu = 1$, $g_0 = 1$, $\eta(\tau) = 1$ -constant internal source
2. $\mu = 1$, $g_0 = 1$, $\eta(\tau) = 1 - cos(\omega\tau)$ -trigonometric internal source
3. $\mu = 1$, $g_0 = 1$, $\eta(\tau) = 200(exp(-0.8\tau) - exp(-0.82\tau)) - 0.3134(\frac{\tau}{4})^2$-exponential internal source.

3. The Chebyshev pseudospectral method's solution process

A detailed, step-by-step guide for applying the CPM method to address a time-dependent heat transfer problem in a longitudinal functionally graded flat fin with a sectional dimension that is unchanged:

Problem statement: Determine the definition of the time-dependent heat transport problem for the longitudinal functional grade flat fin with unchanging cross-sectional area. Specify the governing partial differential equation (PDE), initial conditions, boundary conditions, and any relevant physical characteristics like heat conductivity, fin length, and boundary temperatures.

Mathematical model: Develop the mathematical model describing the time-dependent heat transfer through the fin. The following is a representation of the controlling PDE for the temporary heat transmission:

$$\frac{\partial\theta}{\partial\tau} = aexp(-ax)\frac{\partial\theta}{\partial x} + exp(-ax)\frac{\partial^2\theta}{\partial x^2} - exp(-2ax)N_c\theta + exp(-2ax)G(x,\tau)$$

where θ is the temperature, τ is time, $G(x,\tau) = g_0\eta(\tau)exp(-\mu x)$ is the source function. Here, $g_0 = \frac{b^2(1-R)\mu I_r}{k_0(T_b-T_s)}$ and $\eta(\tau) = \frac{I(\frac{\rho_0 c_0 b^2}{k_0}\tau)}{I_r}$.

Boundary conditions: Specify the first circumstances pertaining to the temperature dispersion at $\tau = 0$ and the boundary conditions for the problem. These typically include the temperatures at the base and tip of the fin in terms of nondimensional form:

$\theta(x,0) = 0\,, \quad \theta(0,\tau) = 1\,, \quad \frac{\partial\theta}{\partial x}(0,\tau) = 0$

Discretization: Discretize the spatial domain (fin length) using Chebyshev nodes. The Chebyshev nodes are given by:

$x_j = \frac{1}{2}[1 - cos(\frac{j\pi}{N}]$

where $j = 0\cdots N$ bounds of the domain, and N is the total amount of nodes. D refers to the Chebyshev differentiation matrices that are built using these points. A grid function ϑ defined at Chebyshev yields a discrete derivative Ω in two steps.

- P must be the sole polynomial of degree $\leq N$ that satisfies $P(x_j) = \vartheta_j$ for $0 < j < N$.
- Assign $P'(x_j)$ to Ω_j .

This process can be described by multiplying a $(N+1)\times(N+1)$ matrix because it is linear. Now let us introduce equations 8, 9, and 10 in their semidiscrete form, which were produced by using matrix D for discrete differencing. Remember that if $\boldsymbol{\vartheta} = [\vartheta_0, \vartheta_1, \cdots, \vartheta_N]^T$ represents a vector of values at positions x_j, with $0 < j < N$, and D, a matrix indicating first order differentiation, then considering $\vartheta'(x_j), \vartheta''(x_j), \ldots$, yields remarkably accurate approximations to $\vartheta'(x_j) = (D\vartheta)_j$, $\vartheta''(x_j) = (D^2\vartheta)_j$, and so on.

Now, we will discretize problems 8, 9, and 10, using the CPM. Regarding the first derivative

$$\begin{bmatrix} \frac{\partial\theta(x_0,\tau)}{\partial x} \\ \frac{\partial\theta(x_1,\tau)}{\partial x} \\ \vdots \\ \frac{\partial\theta(x_N,\tau)}{\partial x} \end{bmatrix} \approx D \begin{bmatrix} \theta(x_0,\tau) \\ \theta(x_1,\tau) \\ \vdots \\ \theta(x_N,\tau) \end{bmatrix} \tag{11}$$

A similar procedure leads to

$$\begin{bmatrix} \frac{\partial^2\theta(x_0,\tau)}{\partial x^2} \\ \frac{\partial^2\theta(x_1,\tau)}{\partial x^2} \\ \vdots \\ \frac{\partial^2\theta(x_N,\tau)}{\partial x^2} \end{bmatrix} \approx D^2 \begin{bmatrix} \theta(x_0,\tau) \\ \theta(x_1,\tau) \\ \vdots \\ \theta(x_N,\tau) \end{bmatrix} \tag{12}$$

Pseudospectral approximation: Approximate the temperature distribution $\theta(x,\tau)$ using Chebyshev polynomials:

$$\theta(x,\tau) \approx \sum_{k=0}^{N} C_k \theta(x_k,\tau)$$

where C_k are the coefficients to be determined.

Collocation method: Apply the collocation method to enforce the time-dependent PDE at the Chebyshev nodes and at each time step. This involves evaluating the time derivative and the spatial derivative terms at each collocation point and setting them equal to the corresponding terms in the PDE.

System of equations: After applying the collocation method, you obtain a system of equations according to the Chebyshev polynomial expansion's coefficient at every time step.

Except for the approximation error in the semidiscrete Chebyshev approximation for 8, 9, and 10, the approximation $\theta(x_i,\tau)$ reduces to a system of $N-1$ ODEs represented by θ_i.

$$\frac{d\theta}{d\tau} = A\theta + B \tag{13}$$

$$\theta(0) = [\theta_1(\tau), \theta_2(\tau), \ldots, \theta_{N-1}(\tau)]^T \tag{14}$$

Here $A = \exp(-ax)D^2 + a\exp(-ax)D - \exp(-2ax)N_c$ is derived from equation 8 and B is evaluated from boundary conditions and source function $G(x,\tau)$ 9 and 10 [5, 27].

Time integration: Use a time integration scheme to evolve the system of equations forward in time. This can be done by solving the system of equations at each time step using a fourth-order Runge-Kutta iterative solver or numerical methods such as matrix inversion, LU decomposition. In the present work, a fourth-order Runge-Kutta iterative solver is used.

Postprocessing: Once you have the coefficients, use them to reconstruct the temperature distribution $\theta(x,\tau)$ throughout the fin. You can then analyze the temperature profile and extract relevant information such as transient temperature profiles, heat fluxes, and thermal behavior of the fin over time.

Validation and interpretation: Validate your results by comparing them to analytical solutions, experimental data, or results from other numerical methods. Interpret within the problem's context, a temporary distribution of temperatures and draw conclusions about the time-dependent heat transport behavior of the fin.

The relative error for a numerical solution can be expressed as follows.

$$\left| \frac{\text{Analytical} - \text{Numerical}}{\text{Analytical}} \right| \tag{15}$$

However, equation 8 with conditions 10 in this study cannot be solved analytically. As a result, the steady-state solution is employed as an analytical method for relative inaccuracy to compare and validate the present results.

When homogeneous material ($a = 0$) is used, the steady-state solution is found as follows

$$\theta(x) = 0.324027e^{x} + 0.324027e^{-x} \tag{16}$$

under the conditions of no internal source ($g_0 = 0$) and $N_c = 1$.

By following these steps, you should be able to effectively use the Chebyshev pseudospectral method to solve the time-dependent heat transport problem for a longitudinal functional grade flat fin with constant cross-sectional area. Notable references, such as Trefethen [27], provide information on how to calculate the Chebyshev differentiation matrix and codes as m-files.

4. Numerical results

This study investigates the behaviour of heat conduction for various homogeneity parameters (a) in the FG longitudinal fin using a time-dependent laser heat source. If the homogeneity indices are assumed to be the same for all properties varying along the axial coordinate, it becomes possible to focus on the homogeneity effect. Thus, the fact that $a = 0$ indicates a homogeneous solution can be easily understood. It is observed that positive values of the inhomogeneity parameter indicate the opposite, i.e. larger values of density, specific heat and thermal conductivity near the outer surface of the medium.

A numerical experiment was performed to investigate the dispersion of temperatures over time as a function of the specific heat source capacity, using $a = 1$. In certain solutions, various μ values were also used to determine specific model properties. The results were analytically verified for the steady state using $N_c = 1$ for the homogeneous case and the relationships are shown in Table 1. The results were obtained at the collocation points determined by dividing the region into 5 parts. As can be seen from Table 1, there is a significant degree of precision and good agreement between the results.

Table 1. Comparison of present results with steady state solution for homogeneous material ($a = 0$) with $g_0 = 0$ and $N_c = 1$.

x	Present results ($\tau = 5$)	Steady state solution	Relative error
0	0.6480545232	0.6480542738	3.848×10^{-7}
0.2	0.6610588577	0.6610586205	3.589×10^{-7}
0.4	0.7005937726	0.7005935709	2.878×10^{-7}
0.6	0.7682459476	0.7682458010	1.908×10^{-7}
0.8	0.8667305098	0.8667304328	8.883×10^{-8}
1	1	1	0

Figure 1 illustrates the temperature distribution on the longitudinal fin without a heat source for five different dimensionless times $\tau = 0.1, 0.3, 0.7, 1.0$ for $a = 1$ for the variation of k only and for the variation of all three of k, c, ρ. Analysis of Figure 1 reveals that the temperature values at the tip of the airfoil become much more extreme over time when only k is varied, compared to when k, c, ρ are all varied. This is clearly a situation that must be considered in the design parameters of the fin.

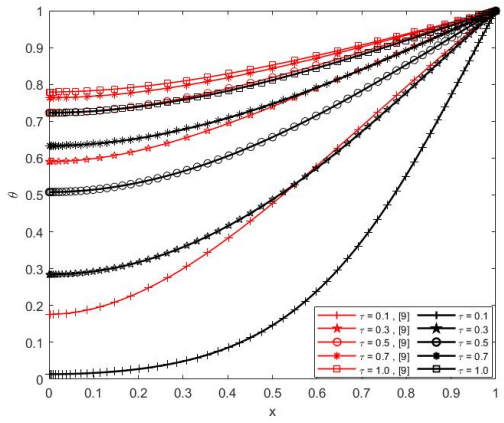

Figure 1. Comparison of k, c, ρ with only k changing state.

The range of temperatures in a functionally graded longitudinal fin under a constant heat source force $(\eta(\tau) = 1)$ is presented in Figures 2–4. Figure 2 shows the change of the dimensionless temperature of a functionally graded fin at some axial points $x = 0.0, 0.3, 0.6$ with time. It has been noted that as time passes, the fin is more affected by the heat source.

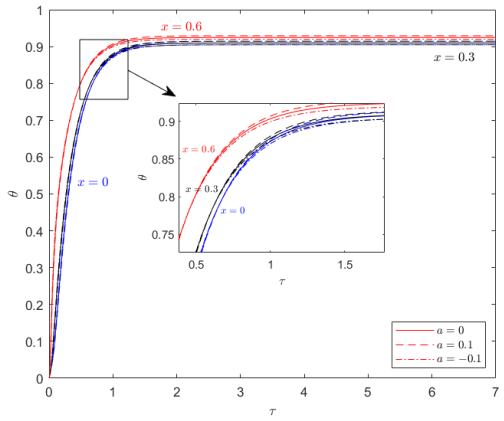

Figure 2. Temperature distribution in a functionally graded longitudinal fin under a constant heat source force $(\eta(\tau) = 1)$ for $x = 0, 0.3, 0.6$.

Furthermore, a correlation has been noted between the homogeneity parameter and the dimensionless temperature. The temperature distributions on the fin are shown in Figures 3 and 4 for three different time values $\tau = 0.1, 0.3, 0.6$ and three different parameters $\mu = 0.3, 1, 3$ at $\tau = 0.3$, respectively. Observations show that for all three time periods, the temperature falls along the fin with an increase in the homogeneity parameter. As the time increases, the temperature at the tip of the blade increases. The temperature decreases as the μ parameter increases and also decreases as the homogeneity parameter increases.

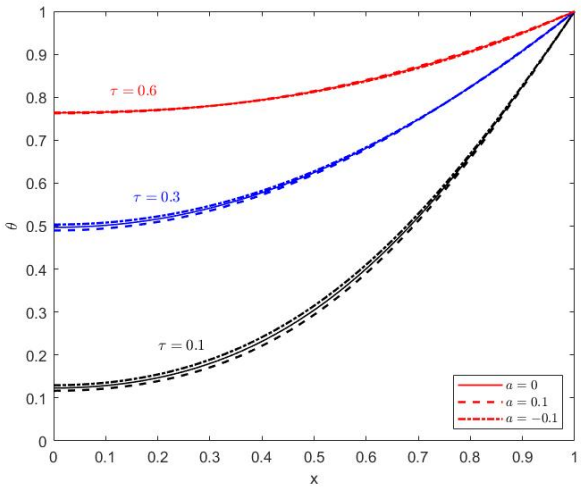

Figure 3. Temperature distribution in a functionally graded longitudinal fin under a constant heat source force $(\eta(\tau) = 1)$ for $\tau = 0.1, 0.3, 0.6$.

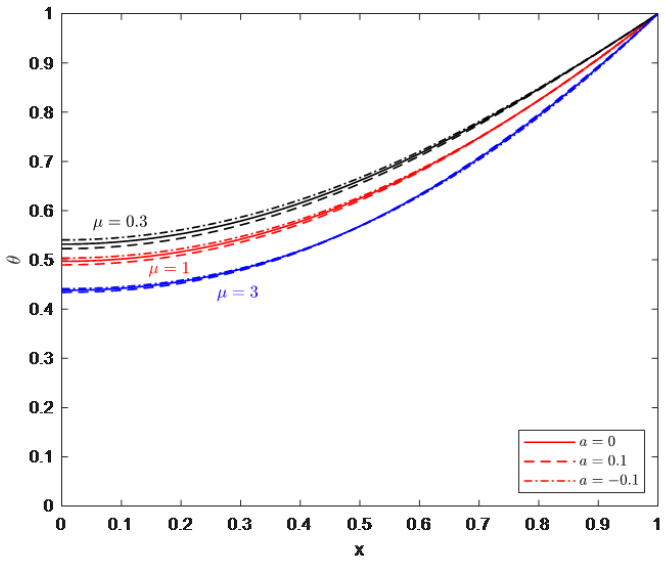

Figure 4. Temperature distribution in a functionally graded longitudinal fin under a constant heat source force $(\eta(\tau) = 1)$ for $\mu = 0.3, 1, 3$ at $\tau = 0.3$.

Figures 5–7 demonstrate the impact of the homogeneity parameters on the dimensionless temperature distribution for the periodic source $\eta(\tau) = 1 - cos\omega\tau$. Figure 5 demonstrates that the amplitude of the time-varying oscillations in temperature decreases as it moves through the medium.

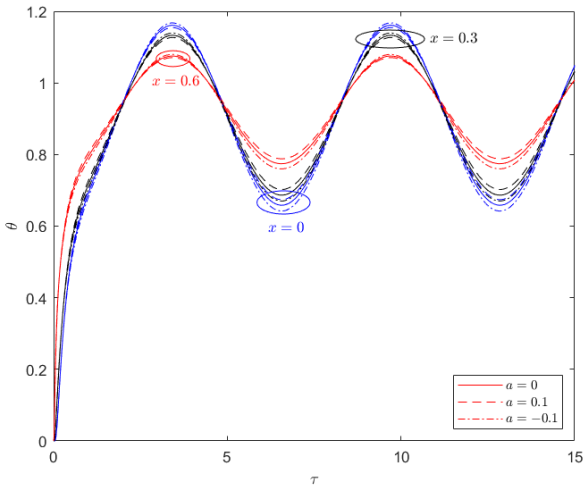

Figure 5. Temperature distribution in a functionally graded longitudinal fin under the effect of a periodic heat source $(\eta(\tau) = 1 - cos\omega\tau)$ for $x = 0, 0.3, 0.6$.

The change in temperature along an axis for three different time levels $\tau = 0.1, 0.3, 0.6$ is shown in Figures 6 and 7 for three different parameters $\mu = 0.3, 1, 3$ at $\tau = 0.3$, respectively. The temperature decreases along the blade for all three time values as the homogeneity parameter increases. As the time increases, the temperature at the tip of the blade increases. The temperature declines as the μ parameter increases and also declines as the homogeneity parameter rises.

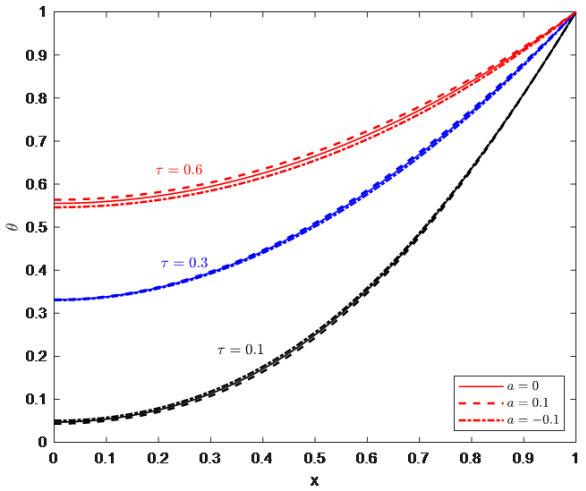

Figure 6. Temperature distribution in a functionally graded longitudinal fin under the effect of a periodic heat source $(\eta(\tau) = 1 - cos\omega\tau)$ for $\tau = 0.1, 0.3, 0.6$.

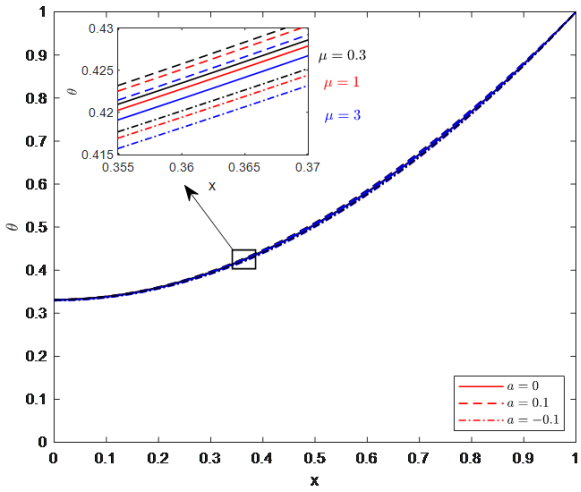

Figure 7. Temperature distribution in a functionally graded longitudinal fin under the effect of a periodic heat source $(\eta(\tau) = 1 - cos\omega\tau)$ for $\mu = 0.3, 1, 3$ at $\tau = 0.3$.

The time variant in temperature at four dissimilar frequencies of the periodic source $\omega = 0.0, 0.1, 0.5, 1.0$ is shown in Figure 8. From this figure, it is evident that the frequency (ω) of the features of the heat source time determines the amplitude and frequency of the temperature oscillations.

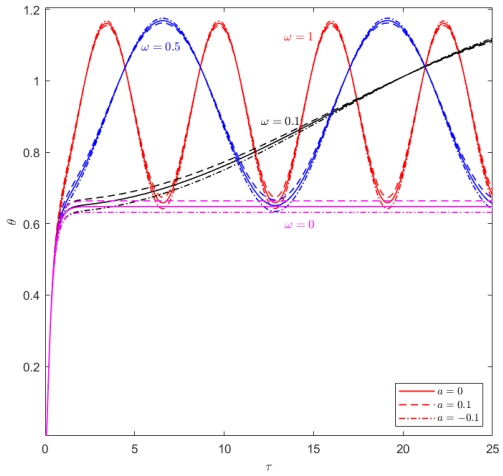

Figure 8. Temperature distribution in a functionally graded longitudinal fin under the effect of four different frequencies of the periodic heat source $(\eta(\tau) = 1 - cos\omega\tau)$ for $\omega = 0.0, 0.1, 0.5, 1.0$ and $x = 0$.

For the exponential source $\eta(\tau) = 200(exp(-0.8\tau) - exp(-0.82\tau)) - 0.3134(\frac{\tau}{4})^2$, Figures 9–11 show how the homogeneity parameters affect the dimensionless temperature distribution. Figure 9 illustrates how the temperature oscillations exhibit a decreasing amplitude as they pass through the medium.

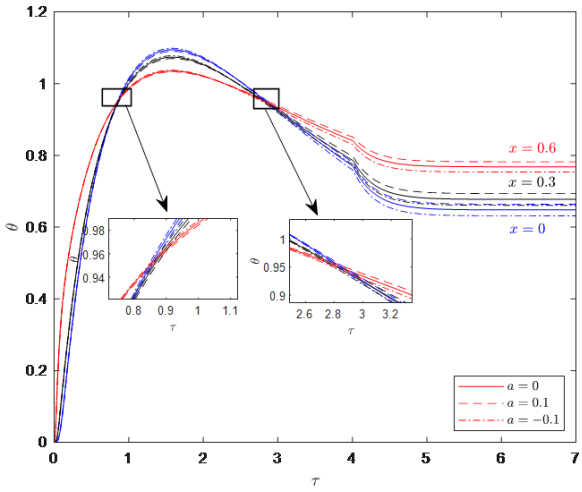

Figure 9. Temperature distribution in a functionally graded longitudinal fin under exponential internal heat source force ($\eta(\tau) = 200(exp(-0.8\tau) - exp(-0.82\tau)) - 0.3134(\frac{\tau}{4})^2$) for $x = 0, 0.3, 0.6$.

Figures 10 and 11, for three distinct time levels $\tau = 0.1, 0.3, 0.6$ and three different parameters $\mu = 0.3, 1, 3$ at $\tau = 0.3$, respectively, display the temperature fluctuation in the axial direction. For all three time values, the temperature drops along the blade as the homogeneity constraint arises. The temperature at the blade's tip rises with increasing time. As the μ constraint increases, the temperature decreases. Similarly, as the homogeneity parameter increases, the temperature also decreases.

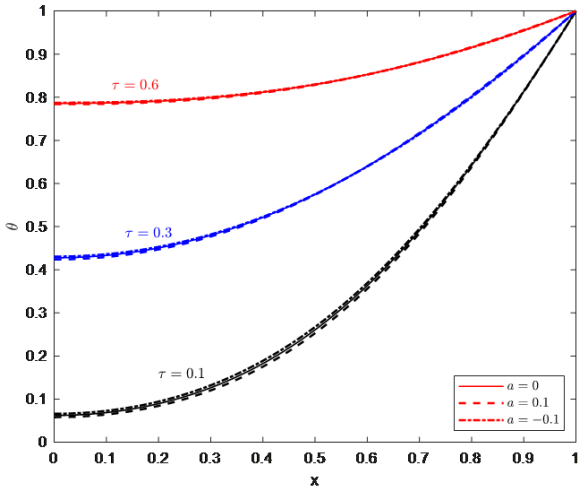

Figure 10. Temperature distribution in a functionally graded longitudinal fin under exponential internal heat source force ($\eta(\tau) = 200(exp(-0.8\tau) - exp(-0.82\tau)) - 0.3134(\frac{\tau}{4})^2$) for $\tau = 0.1, 0.3, 0.6$

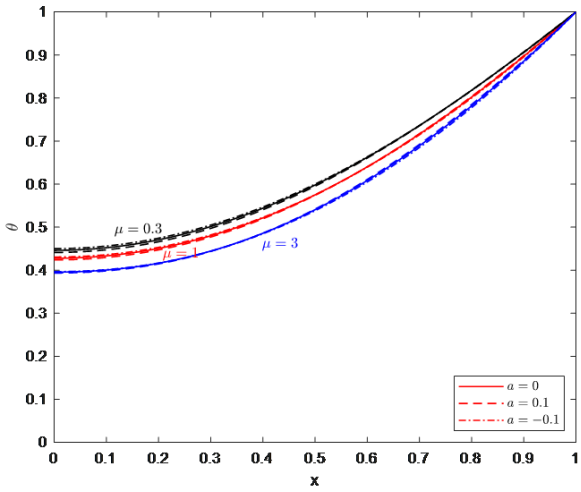

Figure 11. Temperature distribution in a functionally graded longitudinal fin under exponential internal heat source force ($\eta(\tau) = 200(exp(-0.8\tau) - exp(-0.82\tau)) - 0.3134(\frac{\tau}{4})^2$) for $\mu = 0.3, 1, 3$ at $\tau = 0.3$.

5. Conclusion

This study uses CPM to solve the semianalytic model of the temperature dispersion in a longitudinal FGM fin under the effect of a laser heat source that changes with time. Presumably, the internal heat source is a transitory laser heating and that the fin's material properties vary axially in an exponential manner, with the exception of the thermal relaxation constraint. The temperature dispersion of the FGM longitudinal fin is investigated for three different laser sources (constant, trigonometric, and exponential). Comparisons of the temperature distributions for the homogeneous material are analytically tabulated for the steady state using $N_c = 1$. Finally, the following conclusions can be drawn.

1. A general resolution for generating transient temperature dispersions in longitudinal fins constructed of FGM is obtained by working CPM for solving the differential equation.

2. High precision, cheap computing cost, and ease of implementation characterize the solution technique.

3. By understanding the temperature distribution, utilizing FGM on the longitudinal fin will be a successful method of reducing thermal stress.

References

[1] Abbasbandy S, Shivanian E. Exact closed form solutions to nonlinear model of heat transfer in a straight fin. International Journal of Thermal Sciences 2017; 116: 45-51. https://doi.org/10.1016/j.ijthermalsci.2017.01.028

[2] Al-Sanea SA, Mujahid AA. A numerical study of the thermal performance of fins with time-dependent boundary conditions, including initial transient effects. Wärme-Und Stoffübertragung 1993; 28: 417-24. https://doi.org/10.1007/BF01577883

[3] Assis E, Kalman H. Transient temperature response of different fins to step initial conditions. International Journal of Heat and Mass Transfer 1993; 36: 4107-4114. https://doi.org/10.1016/0017-9310(93)90072-E

[4] Aziz A, Bouaziz MN. A least squares method for a longitudinal fin with temperature dependent internal heat generation and thermal conductivity. Energy Conversion and Management 2011; 52: 2876-2882. https://doi.org/10.1016/j.enconman.2011.04.003

[5] Bazan NG. Neurotrophins induce neuroprotective signaling in the retinal pigment epithelial cell by activating the synthesis nl of the anti-inflammatory and anti-apoptotic neuroprotectin D1. Recent Advances in Retinal Degeneration 2008; 39-44. https://doi.org/10.1007/978-0-387-74904-4_3

[6] Beckett PM. High-intensity laser-induced vaporization without internal superheating. Journal of Applied Physics 1985; 58: 2943-2948. https://doi.org/10.1063/1.335842

[7] Chiu CH, Chen CK. A decomposition method for solving the convective longitudinal fins with variable thermal conductivity. International Journal of Heat and Mass Transfer 2002; 45: 2067-2075. https://doi.org/10.1016/S0017-9310(01)00286-1

[8] Cuce E, Cuce PM. Homotopy perturbation method for temperature distribution, fin efficiency and fin effectiveness of convective straight fins with temperature-dependent thermal conductivity. Proceedings of the Institution of Mechanical Engineers Part C Journal of Mechanical Engineering Science 2013; 227: 1754-1760. https://doi.org/10.1177/0954406212469579

[9] Demir H, Sungu IC, Keles I. Unified approach for transient heat transfer in a longitudinal fin with functional grading. The European Physical Journal Plus 2023; 138: 430. https://doi.org/10.1140/epjp/s13360-023-04031-z

[10] Gardner KA. Efficiency of extended surface. Transactions of the American Society of Mechanical Engineers 1945; 67: 621-628. https://doi.org/10.1115/1.4018343

[11] Ghasemi SE, Hatami M, Ganji DD. Thermal analysis of convective fin with temperature-dependent thermal conductivity and heat generation. Case Studies in Thermal Engineering 2014; 4: 1-8. https://doi.org/10.1016/j.csite.2014.05.002

[12] Gottlieb D, Orszag SA. Numerical Analysis of Spectral Methods. Philadelphia, PA, USA: SIAM; 1977.

[13] Harper RR, Brown WB. Mathematical equations for heat conduction in the fins of air-cooled engines. NACA Technical Reports, 1923.

[14] Irandegani A, Sanjaranipour M, Sarhaddi F. Thermal performance evaluation of longitudinal fins with various profiles using homotopy perturbation method. Iranian Journal of Science and Technology, Transactions A: Science 2020; 44: 1761-1774. https://doi.org/10.1007/s40995-020-00973-6

[15] Jaya Krishna D. Operational time and melt fraction based optimization of a phase change material longitudinal fin heat sink. Journal of Thermal Science and Engineering Applications 2018; 10: 64502. https://doi.org/10.1115/1.4040988

[16] Jayaprakash MC, Alzahrani HAH, Sowmya G, Kumar RSV, Malik MY et al. Thermal distribution through a moving longitudinal trapezoidal fin with variable temperature-dependent thermal properties using DTM-Pade approximant. Case Studies in Thermal Engineering 2021; 28: 101697. https://doi.org/10.1016/j.csite.2021.101697

[17] Khan WA, Aziz A. Transient heat transfer in a functionally graded convecting longitudinal fin. Heat and Mass Transfer 2012; 48: 1745-1753. https://doi.org/10.1007/s00231-012-1020-z

[18] Lewandowska M. Hyperbolic heat conduction in the semi-infinite body with a time-dependent laser heat source. Heat and Mass Transfer 2001; 37: 333-342. https://doi.org/10.1007/s002310000176

[19] M Al-Makhyoul Z. Heat characteristics and performance of longitudinal fin exposed to wet air. AL-Rafdain Engineering Journal 2014; 22: 176-185. https://doi.org/10.33899/rengj.2014.88463

[20] Mosayebidorcheh S, Farzinpoor M, Ganji DD. Transient thermal analysis of longitudinal fins with internal heat generation considering temperature-dependent properties and different fin profiles. Energy Conversion and Management 2014; 86: 365-370. https://doi.org/10.1016/j.enconman.2014.05.033

[21] Ndlovu PL. The significance of fin profile and convective-radiative fin tip on temperature distribution in a longitudinal fin. Nano Hybrids and Composites 2019; 26: 93-105. https://doi.org/10.4028/www.scientific.net/NHC.26.93

[22] Pan C, Vermaak N, Romero C, Neti S, Hoenig S et al. Efficient optimization of a longitudinal finned heat pipe structure for a latent thermal energy storage system. Energy Conversion and Management 2017; 153: 93-105. https://doi.org/10.1016/j.enconman.2017.09.064

[23] Panahizadeh F, Hasnat M, Ghafouri A. Numerical Modeling of transient heat transfer in longitudinal fin. Analele Universitatii" Eftimie Murgu" Resita. Fascicula de Inginerie 2017; 14: 320-328.

[24] Ready JF. Industrial Applications of Lasers. Elsevier; 1997.

[25] Sobamowo MG. Thermal analysis of longitudinal fin with temperature-dependent properties and internal heat generation using Galerkin's method of weighted residual. Applied Thermal Engineering 2016; 99: 1316-1330. https://doi.org/10.1016/j.applthermaleng.2015.11.076

[26] Sobamowo MG, Oguntala GA, Yinusa AA, Adedibu AO. Analysis of transient heat transfer in a longitudinal fin with functionally graded material in the presence of magnetic field using finite difference method. World Scientific News 2019; 166-187.

[27] Trefethen LN. Spectral Methods in MATLAB. SIAM; 2000.

[28] Varun Kumar RS, Sarris IE, Sowmya G, Prasannakumara BC, Verma A. Artificial neural network modeling for predicting the transient thermal distribution in a stretching/shrinking longitudinal fin. ASME Journal of Heat and Mass Transfer 2023; 145: 83301. https://doi.org/10.1115/1.4062215

[29] Vyas PD, Thakur H, Darji VP. Transient analysis of variable profile longitudinal fin using meshless local Petrov Galerking method (MLPG). International Journal of Applied Engineering Research 2018; 13: 49-55.

[30] Yue TM, Jiang CY, Xu JH, Lau WS. Laser fantasy: from machining to welding. Journal of Materials Processing Technology 1996; 57: 316-319. https://doi.org/10.1016/0924-0136(95)02081-0